Supplementary Material: High Fidelity Manipulation of the Quantized Motion of a Single Atom via Stern-Gerlach Splitting

Kun-Peng Wang (王坤鹏),[1,2,3] Jun Zhuang (庄军),[1,2,3] Xiao-Dong He (何晓东),[1,2,*] Rui-Jun Guo (郭瑞军),[1,2,3] Cheng Sheng (盛诚),[1,2] Peng Xu (许鹏),[1,2] Min Liu (刘敏),[1,2] Jin Wang (王谨),[1,2] and Ming-Sheng Zhan (詹明生)[1,2,†]

[1] *State Key Laboratory of Magnetic Resonance and Atomic and Molecular Physics, Wuhan Institute of Physics and Mathematics, APM, Chinese Academy of Sciences, Wuhan 430071, China*

[2] *Center for Cold Atom Physics, Chinese Academy of Sciences, Wuhan 430071, China*

[3] *University of Chinese Academy of Sciences, Beijing 100049, China*

A. Analysis of the experimental fluctuations

In this section we describe in detail the comparison between the measured fidelity of the sideband π-transitions and the simulations of this transition and the Randomized benchmarking. To this end, we firstly extract the fluctuations of the experimental conditions and using these obtained parameters to perform further simulations of the fidelity. We distinguish the short-term fluctuations on time scales of 10 s and the long term drifts on time scales of 1000 s of the magnetic field and microwave power. To extract the fluctuations we perform Mont-Carlo simulations to fit the experimental data of Rabi oscillations.

The microwave radiation induces transitions between the $|2,-2\rangle$ state accompanied with motional state $|n\rangle$ and $|1,-1\rangle$ in motional state of $|n'\rangle$. The quantum states can be denoted by $|\psi\rangle = \begin{pmatrix} c_2 \\ c_1 \end{pmatrix}$, where c_2 and c_1 are the probability amplitude in the $|2,-2\rangle$ and $|1,-1\rangle$ states respectively. The atoms initially starts from $|2,-2\rangle$ i.e. $\begin{pmatrix} 1 \\ 0 \end{pmatrix}$. Then the time evolution under the microwave pulse can be described by $\begin{pmatrix} c_2(t) \\ c_1(t) \end{pmatrix} = \mathbf{M} \cdot \begin{pmatrix} c_2(0) \\ c_1(0) \end{pmatrix}$ with the matrix of [1]

$$\mathbf{M} = \begin{pmatrix} \exp\left(i\frac{\Delta t}{2}\right)\left[\cos\left(\frac{\Omega' t}{2}\right) - i\frac{\Delta}{\Omega'}\sin\left(\frac{\Omega' t}{2}\right)\right] & i\exp\left(i\frac{\Delta t}{2}\right)\frac{\Omega^*}{\Omega'}\sin\left(\frac{\Omega' t}{2}\right) \\ i\exp\left(-i\frac{\Delta t}{2}\right)\frac{\Omega}{\Omega'}\sin\left(\frac{\Omega' t}{2}\right) & \exp\left(-i\frac{\Delta t}{2}\right)\left[\cos\left(\frac{\Omega' t}{2}\right) + i\frac{\Delta}{\Omega'}\sin\left(\frac{\Omega' t}{2}\right)\right] \end{pmatrix} \tag{A1}$$

, where Δ is the microwave detuning of the resonant transitions, Ω is the Rabi frequency of the resonant microwave transitions which is proportional to the square root of the microwave power, and ω' is the generalized Rabi frequency $\Omega' = \sqrt{\Omega^2 + \Delta^2}$. The resonant microwave frequency is scanned detuning at a fixed pulse duration such as 0.03 ms for the carrier transitions of $|2,-2\rangle \bigotimes |0\rangle \rightarrow |1,-1\rangle \bigotimes |0'\rangle$. The actual detuning Δ will be affected by an external magnetic field and changes the atomic energy levels due to the Zeeman effect. To create a low-noise and stable magnetic field we use an ultra low-noise current supply and synchronize the experiments with the ac lines to suppress the influence of 50 Hz magnetic field. And the generalized Rabi frequency Ω' will be affected both the fluctuations on the magnetic field and microwave power or the Rabi frequency Ω.

* hexd@wipm.ac.cn

† mszhan@wipm.ac.cn

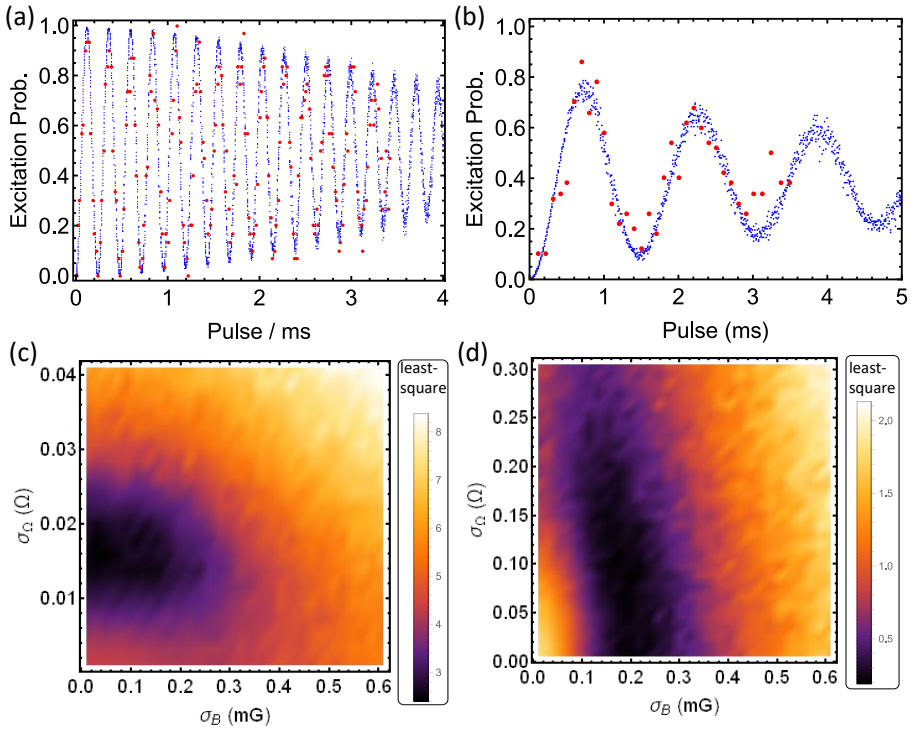

Figure S1. Rabi oscillations and simulations. In (a) and (b), the carrier and third-order sideband transitions are driven as a function of microwave pulse durations respectively. The experimental data points are shown with red points and simulations are shown with blue points. Each point is obtained by averaging over 50 runs of experiments. The Monte Carlo simulations in the conditions of $\{\sigma_B = 0.19$ mG, $\sigma_\Omega = 0.012\ \Omega\}$. In (c) and (d), the least square values are shown as a function of σ_B and σ_Ω with the corresponding Rabi frequencies as input parameters. The minimum of σ_Ω and σ_B are obtained from (c) and (d) respectively.

To extract the fluctuations experienced by the atoms, as shown in Fig. S1, we measure the Rabi oscillations of the $|2,-2\rangle \bigotimes |0\rangle \rightarrow |1,-1\rangle \bigotimes |0'\rangle$ transition and the $|2,-2\rangle \bigotimes |0\rangle \rightarrow |1,-1\rangle \bigotimes |3'\rangle$ transition which has a relative small Rabi frequency of $\Omega_{sb3} = 2\pi \times 0.618(8)$ kHz. We model the noise of the magnetic field and microwave power with a white noise model that have the form of Gaussian (normal) distribution of $f(x) = \exp\left(-\frac{(x-\mu_f)^2}{2\sigma_f^2}\right)$ ($f = B$ or Ω), where μ_f is the mean value and σ_f is the standard deviation. And we suppose that the scaling factor between the Rabi frequency Ω and the square root of the microwave power $\sqrt{P}$ is a constant f_c (f_{sb}) for the carrier (sideband) transition. Thus the relative fluctuation on the Rabi frequency $\sigma_{\Omega_c}/\Omega_c$ for the carrier transition is equivalent to $\sigma_{\Omega_{sb}}/\Omega_{sb}$ for the sideband transitions. So we express the microwave power fluctuation as $\sigma_\Omega \propto \Omega$ and omit the subscripts for simplicity. The corresponding two-dimensional simulations as functions of σ_B and σ_Ω are shown in Fig. S1(c) and (d) respectively. We extract $\sigma_\Omega = 0.012(1)\ \Omega$ from Fig. S1(c) and $\sigma_B = 0.19(1)$ mG from Fig. S1(d). We note that, from Fig. S1(c), the fitted $\sigma_B = 0.00(2)$ mG is unphysical. The simulated Rabi oscillations of the carrier and third-order sideband transitions under the condition of $\{\sigma_B = 0.19$ mG, $\sigma_\Omega = 0.012\ \Omega\}$ are shown in Fig. S1(a) and (b) respectively.

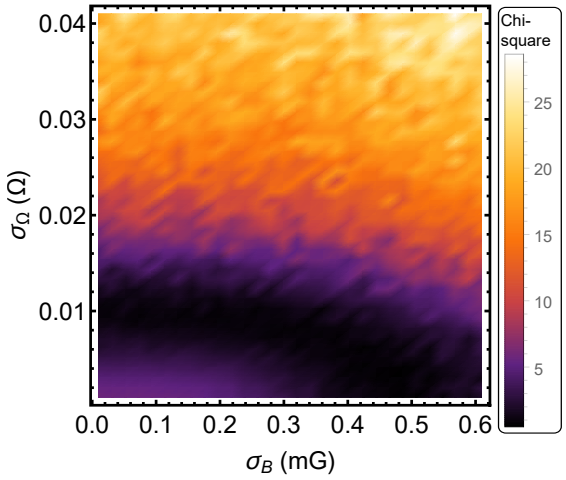

Figure S2. The Monte Carlo simulations of the multi-pulse sequence. The chi-square values are shown for different settings of $\{\sigma_B, \sigma_\Omega\}$. For $\sigma_\Omega = 0.012$ Ω, the σ_B has a relative broad range of small chi-squares.

B. Simulation of the π-pulse transition and the RB sequence

To determine the fidelity of the motional state control, we apply a multi-π pulse sequence as described in the main text. Rather than performing the standard randomized benchmarking, we extract the fidelity by an analytical fitting and comparing with Monte Carlo simulations. We perform two-dimensional simulations for different values of $\{\sigma_B, \sigma_\Omega\}$, as shown in Fig. S2, which have a broad parameter range. Thus we do not fit the fluctuations of magnetic field and microwave power in this data set but derive them from Rabi oscillations as described previously. And we simulate the multi-π pulse sequence with the derived parameters which agree well with the experimental measurements as shown in Fig. 4 (a) of the main text. The fidelity between two density matrices ρ and σ is defined as $F(\rho, \sigma) = (\mathrm{Tr}\sqrt{\sqrt{\rho}\sigma\sqrt{\rho}})^2$. We denote ρ as the density matrix of the target state and σ as the final state after the experimental sequence. We simulate 10000 random samples for different set of magnetic field noise while keep $\sigma_\Omega = 0.012$ Ω. The simulated fidelities are obtained from fitting of histogram counts of the simulated data points and the error is denote as the 1σ width of the fitted curve. For the specific condition of $\sigma_B = 0.19$ mG, as shown in Fig. S3, the obtained fidelity is 0.9973(3) with an error of $3E-4$. The σ_B-dependent simulation results are depicted in Fig. 4 (b) of the main text. Before we upgrade the current supply that generates the magnetic field, the σ_B is fitted to be 0.57 mG, and the obtained π-pulse fidelity is 0.981(3). After upgrading the current supply, the fidelity is raised to 0.996(1).

In Fig. 4 (b), the measured fidelities of the π-transition are smaller than the Monte Carlo simulations, it may because the noise model used in the simulations are not very precise especially for long term drifts. The long term drift of the magnetic field can be determined by monitoring the resonant transition frequency. The microwave transition frequency drifts about 0.8 kHz on a typical time scale of 1000 s, which corresponds to magnetic field drift of 0.4 mG. The drift of the microwave power can be determined by measuring the accurate π-pulse duration. The drift is about 0.01 times the π-pulse duration. The long term drifts could cause an offset in the pulse area which could lead to error cancellations in the multi-π sequence. As shown in Fig. S4, if there is a constant offset in the pulse duration, the error cancellation will appear as an oscillating probability as a of function pulse number. In experiment, these long-term drifts can be bypassed by calibrating experimental

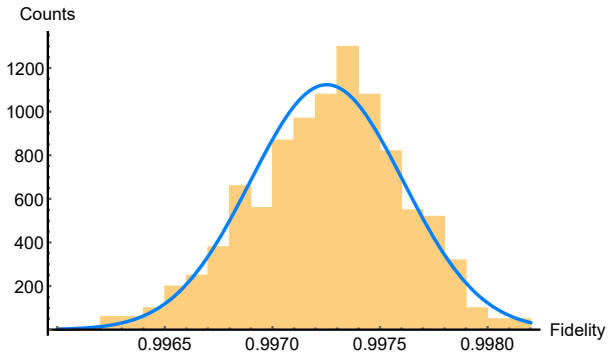

Figure S3. The histogram of the Monte Carlo simulations of the sideband π-pulse fidelity for $\{\sigma_B = 0.19$ mG, $\sigma_\Omega = 0.012\ \Omega\}$.

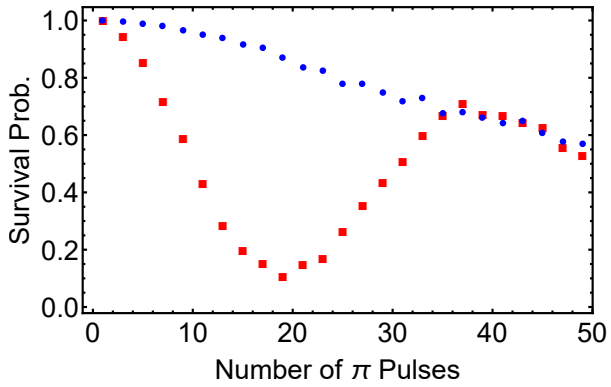

Figure S4. The error cancellation behavior. The red squares are the simulated results with a constant pulse duration error of $0.05\tau_\pi$ in the condition of $\{\sigma_B = 0.19$ mG, $\sigma_\Omega = 0.012\ \Omega\}$. τ_π is the π-pulse duration. When the offset error is set to $0.004\tau_\pi$, as filled circles shown, the error cancellation could be effectively suppressed.

parameters frequently (as filled circles shown in Fig. S4). The effect of residual drifts may still affect the measured fidelity after calibration, but the error cancellation does not emerge obviously in the multi-pulse measurement in Fig. 4 (a) in the main text.

Different single-qubit gates have different sensitivity to experimental fluctuations. The average fidelity of single qubit gates in a Clifford group is typically obtained by performing randomized benchmarking (RB) [2]. In RB, 24 single-qubit Clifford gates are applied in random sequences to estimate the average gate errors, where the definition of the gates can be fond in ref. [3]. Starting from one qubit state $|0\rangle$, the RB sequences are introduced and end up with a final gate to flip the qubit state, in the ideal case without errors, to $|1\rangle$. The resulting probabilities in $|1\rangle$ decay exponentially with the number of gates l as [2]

$$P = \frac{1}{2} + \frac{1}{2}(1 - d_{if})(1 - 2\epsilon)^l \tag{A2}$$

, where d_{if} is the depolarization probability associated with state preparation, measurement, and the final transfer gate, while ϵ is the average error per gate. The average fidelity of a Clifford gate is $\overline{F} = 1 - \epsilon$, where ϵ is the corresponding error.

We perform Monte Carlo simulations of RB and obtain average fidelities for different experimental fluctuations which are shown in Fig. S3. For the specific case of $\{\sigma_B = 0.19$ mG, $\sigma_\Omega = 0.012\ \Omega\}$, the simulation results and its fitting are shown in Fig. S5, leading to an average fidelity of 0.995(2). Due to the sensitivity to

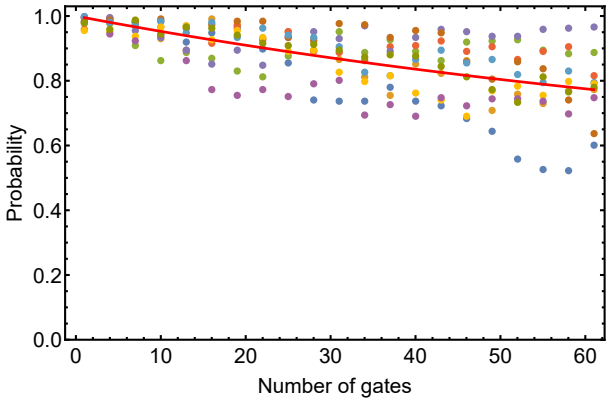

Figure S5. The Monte Carlo simulations of the randomized benchmarking with 24 single-qubit Clifford gates. σ_Ω is set to 0.012 Ω and σ_B is set to 0.19 mG. The randomized gates are applied in ten different random sequence. The solid curve is a fit to Equation (A2) of the average probabilities at each number of gates, the average values and corresponding standard deviations are not shown. The resulting average fidelity is 0.995(2) corresponding to an average error of 0.005(2).

errors of pulse area and phase coherence of the Clifford gates, the average fidelities in RB are typically lower than the calculated π-pulse fidelities and the standard deviations of the average fidelities are also larger than π-pulse fidelities.

[1] Saffman M and Walker T G 2005 *Phys. Rev. A* **72** 022347

[2] Knill E, Leibfried D, Reichle R, Britton J, Blakestad R B, Jost J D, Langer C, Ozeri R, Seidelin S and Wineland D J 2008 *Phys. Rev. A* **77** 12307

[3] Xia T, Lichtman M, Maller K, Carr A W, Piotrowicz M J, Isenhower L and Saffman M 2015 *Phys. Rev. Lett.* **114** 100503